

Comparative genomics study of inverted repeats in bacteria

Fabrizio Lillo *, Salvatore Basile *,† and Rosario N. Mantegna *,†

*Istituto Nazionale per la Fisica della Materia, Unità di Palermo, Viale delle Scienze, I-90128, Palermo, Italia

† Dipartimento di Fisica e Tecnologie Relative, Università di Palermo, Viale delle Scienze, I-90128 Palermo, Italia

We investigate the number of inverted repeats observed in 37 complete genomes of bacteria. The number of inverted repeats observed is much higher than expected using Markovian models of DNA sequences in most of the eubacteria. By using the information annotated in the genomes we discover that in most of the eubacteria the inverted repeats of stem length longer than 8 nucleotides preferentially locate near the 3' end of the nearest coding regions. We also show that IRs characterized by large values of the stem length locate preferentially in short non-coding regions bounded by two 3' ends of convergent genes. By using the program TransTerm recently introduced to predict transcription terminators in bacterial genomes, we conclude that only a part of the observed inverted repeats fulfills the model requirements characterizing rho-independent termination in several genomes.

An inverted repeat (IR) in DNA sequences provide the necessary condition for the potential existence of a hairpin structure in the transcribed messenger RNA and/or cruciform structures in DNA [1]. Inverted repeats play an important role for regulation of transcription and translation. Examples are the role of the IR located in the promoter region of the S10 ribosomal protein operon [2–4] and the role of IR in the *lac* operator [5,6]. It has also been proposed that hairpins play an important role in the control of transcription, translation and other biological functions [7,8]. Hairpin- or cruciform-binding proteins have been identified from several species. These results suggest that regulatory hairpins may be involved in transcription of a number of genes [9]. The existence in vivo of hairpin structures of messenger RNA during transcription has been demonstrated [10–14]. Hairpin structures are often associated with rho-independent intrinsic terminators of genes in several bacteria. The presence of such intrinsic terminators has been observed in *E. coli* [15]. Rho-independent intrinsic terminators have also been detected in other bacteria as, for example, *Streptococcus pneumoniae* [16], *Pseudomonas aeruginosa* [17], *Myxococcus xanthus* [18], *Streptococcus equisimilis* H46A [19] and *Chromatium vinosum* D [20]. Hairpin structures can occur at the mRNA when an IR is present in the DNA sequence. For example, the sequence 5'aGGAATC-GATCTTaacgAAGATCGATTCCa3' is a sequence having a sub-sequence GGAATCGATCTT which is the IR of AAGATCGATTCC. This IR can form a hairpin having a stem of length 12 nucleotides and a loop (aacg) of length 4 nucleotide in the transcribed RNA. The number of IRs has been investigated with bioinformatics methods in long DNA sequences of eukaryotic (human and yeast) and bacterial (*E.coli*) DNA [21] and in the complete genomes of eubacterium *Haemophilus influenzae* [22], archaeobacterium *Methanococcus jannaschii* and cyanobacterium *Synechocystis* sp. PCC6803 [23]. These studies have shown that inverted repeats are rather abundant in *E. coli* and *Haemophilus influenzae*, poorly abundant in *Methanococcus jannaschii* and with no enrich-

ment (with respect to a Bernoullian assumption about DNA sequences) in *Synechocystis* [21,23].

DATA AND METHODS

In the present study, we investigate 37 complete genomes of bacteria recently sequenced (all the bacterial complete genomes publicly available at the time of our study). The set consists of 8 archaeobacteria, 1 aquificales, 1 thermotogales, 2 spirochetales, 5 chlamydiales, 1 deinococcus, 1 cyanobacterium, 12 proteobacteria (purple bacteria) and 6 firmicutes (gram positive). The analyzed DNA totals 77.8 millions base pairs. In the completed genomes we search with a specialized computer program all the inverted repeats of stem length ℓ ranging from 4 to 20 and loop (spacer) length m ranging from 3 to 10. These are typical boundaries in the range of the ones used in the literature for the investigation of IRs, in DNA sequences [21,23,24]. The results of our investigation are illustrated in Figure 1 and summarized in Table I. The available genomes differ the one from the other with respect to the CG content and the degree of its fluctuation along the genome. In our study, each detected IR is the IR of maximal stem length ℓ located in a given DNA position. In other words, we check that the first two nucleotides immediately out of the stem region have not a palindromic counterpart for each observed IR. Within this definition, the number of IRs expected in a genome under the simplest assumption of a random Bernoullian DNA is given by the equation

$$n_{ex}(\ell, m) = N(1 - 2P_aP_t - 2P_cP_g)^2 \times (2P_aP_t + 2P_cP_g)^\ell, \quad (1)$$

where N is the number of nucleotides in the genome sequence and P_a , P_c , P_g and P_t are the observed frequencies of nucleotides. Eq. (1) shows that the number of expected IRs is independent of m whereas it depends on the CG content of the genome. The CG content can vary

considerably across different regions of the same genome. Moreover, a Bernoullian description of DNA sequences provides just a rough approximation of the statistical properties observed in real genome. For this reason, we decide to compare the results obtained in real genomes with the ones obtained by generating a computer generated first-order Markov genome having the same probability matrix of dinucleotides empirically observed within each non-overlapping window of 10,000 nucleotides for each genome. The occurrence of IRs detected in the computer generated genomes are used for comparison in Figure 1 and to obtain the χ^2 values used to illustrate the empirical results summarized in Table I.

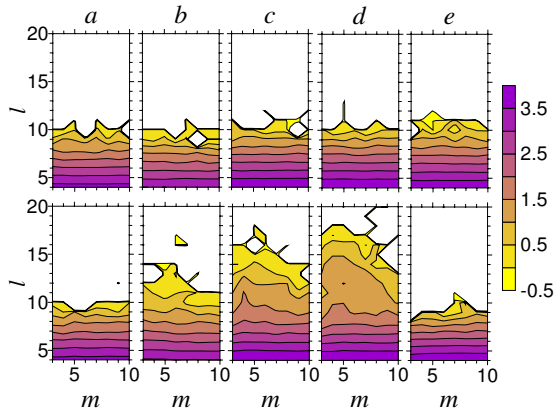


FIG. 1. Contour plot of the decimal logarithm of the total occurrence of IRs of stem length ℓ and loop length m for 5 representative genomes (bottom panels) compared with the decimal logarithmic occurrence of corresponding computer generated first-order Markovian data (top panels). From left to right we show (a) the archaeobacterium *Archaeoglobus fulgidus*, (b) the *Chlamydia pneumoniae* CWL029, (c) the proteobacterium *Escherichia coli*, (d) the firmicute *Bacillus subtilis* and (e) the cyanobacterium *Synechocystis* sp.. The numbers of color scale are decimal logarithm of the total occurrence of IRs.

In Figure 1 we show the contour lines of the decimal logarithm of the number of occurrence of IRs as a function of the stem length ℓ and of the loop length m for 5 representative genomes. To take into account the differences in length, CG content and Markovian characterization observed in the genomes we also show in Figure 1 (top panels of the figure) the results obtained for the same investigation performed with the corresponding computer generated Markovian genomes. The selected genomes are: *Archaeoglobus fulgidus* (archaeobacteria), *Chlamydia pneumoniae* CWL029 (chlamydiales), *Bacillus subtilis* (firmicutes), *Escherichia coli* (proteobacteria) and *Synechocystis* sp. (cyanobacteria). In the absence of the statistical uncertainties detected at the noise level, Markovian generated data show contour lines, which are straight lines parallel to the horizontal axis (loop length

m). This is consistent with the theoretical result of Eq. (1) obtained for a Bernoullian DNA sequence. In fact, the theoretical prediction of Eq. (1) does not depend on m . Moreover, the distance between two successive contour lines is approximately constant. This second observation indicates that, once again consistently with the prediction of Eq. (1), the number of occurrences of inverted repeats exponentially decreases with the stem length ℓ in a local Markov model of DNA sequences. The results obtained in real genomes (bottom panels of Figure 1) are genome dependent. Some genomes as *Archaeoglobus fulgidus* and *Synechocystis* sp. show a general pattern hardly distinguishable from the one observed in computer generated data whereas *Chlamydia pneumoniae* CWL029, *Bacillus subtilis* and *Escherichia coli* are characterized by the occurrence of inverted repeats which are not explained by a first-order Markovian model of DNA. For these three genomes, but they are representative of several others genomes, it is worth noting that the contour lines of Figure 1 show both (i) a value of the occurrence of inverted repeats much larger than expected for a first-order Markovian model for large values of ℓ and (ii) an occurrence of inverted repeats which is strongly dependent on the specific value of m for large values of ℓ . We verify that higher-order Markovian models up to the fifth-order also fail to reproduce these empirical results. In other words these empirical results cannot be ascribed to the strong bias up to the esamer level present in several genomes. In agreement with previous studies devoted to the search of inverted repeats in long DNA sequences (Schroth and Shing Ho, 1995; Cox and Mirkin, 1997) we detect the existence of different levels of enhancement of the number of observed inverted repeats in different species of bacteria. The results presented in Figure 1 are just illustrative of the varied behavior observed in 5 different case. The complete results obtained by our investigation are summarized in Table I where we group the 37 investigated genomes.

RESULTS AND DISCUSSION

In Table I we report the observed number of inverted repeats as a function of the stem length ℓ for each investigated genome. The genomes are listed in groups separated by a horizontal line. From top to bottom, the groups are archaeobacteria, chlamydiales, firmicutes, proteobacteria and others. This last group includes aquificales, spirochetes, deinococcales, cyanobacteria and thermotogales. To limit the size of the Table we sum up the occurrence observed for different values of $3 \leq m \leq 10$. To make comparison possible between genomes of different sizes, the values are normalized to one million base pairs. In the Table we also provide (in parenthesis) the value expected for computer generated genomes characterized by a local first-order Markovian

model. The χ^2 values are calculated by comparing the empirical occurrence of IR with respect to the one predicted by a first-order Markovian process. The χ^2 is calculated by comparing the empirical occurrence of inverted repeats with the occurrence of computer generated data when ℓ is varying from 4 to 20 (the number of IRs with $\ell = 4$ and $\ell = 5$ are not shown in Table I for lack of space. They are available at the web site <http://lagash.dft.unipa.it/IR.html>). The χ^2 calculation is done by comparing the two distributions using six bins. In fact, the number of IRs with $\ell > 8$ are summed up together in the presentation of Table I and in the χ^2 calculation to compensate the exponential decrease observed in the number of IRs when ℓ increases. The obtained χ^2 values are in all except one case larger than 30 implying that the p value is always below (and often much below) 1×10^{-5} . The only exception is the aquificales *Aquifex aeolicus* that present a p value of 0.52. To make a direct comparison between different genomes, in Table I we use a color code for the contribution to the χ^2 of each different number of IRs of stem length ℓ . Specifically, for each value of ℓ we compute $(n_{obs} - n_{Markov})/\sqrt{n_{Markov}}$. The square of this quantity directly contributes to the χ^2 value. In the Table, for values of this parameter lower than -3 we use a blue character. A black character is used when this parameter is between -3 and 3, for values larger than 3 we use a red character and for values larger than 10 the number of IRs is purple.

Our results show that the number of inverted repeats is much higher than the one theoretically expected for a first-order Markovian DNA of the same composition in chlamydiales, firmicutes and proteobacteria. Deviations in the observed number of IRs that contribute more than 100 to the χ^2 are detected in several genomes especially when $\ell > 8$. Moreover, we observe deviations of the number of IRs that contribute more than 9 to the χ^2 in the large majority of genomes for almost all the ℓ values. Among eubacteria only *Aquifex aeolicus* show no enrichment, whereas *Deinococcus radiodurans* and *Synechocystis* sp. show less IRs than predicted by a first-order Markovian DNA. In contrast, a general pattern does not emerge in archaeobacteria. In three of the eight complete genomes investigated the number of empirically observed IRs is comparable with the one expected by using a Markovian model, whereas in the cases of *Aeropyrum pernix*, *Halobacterium* sp., *Methanococcus jannaschii*, *Methanobacterium thermoautotrophicum* and *Thermoplasma acidophilum* IRs are slightly more frequent or more frequent than expected. In spite of this variety of behavior, a general remark is that the number of IRs in archaeobacteria is, in most cases, much lower than the one observed in eubacteria.

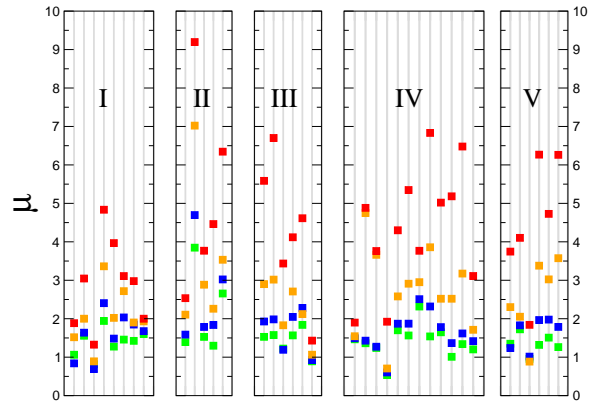


FIG. 2. Ratio μ between the percentage of IRs found in non-coding regions and the percentage of non-coding regions present in the entire genome. Each vertical line refers to a genome. The 37 investigated genomes are grouped as archaeobacteria (I), chlamydiae (II), firmicutes (III), proteobacteria (IV) and others (V). Within each group, the order of the different genomes is the same as the one given in Table I. Different colors of the symbol refer to different values of ℓ . Specifically, we use green for $\ell = 6$, blue for $\ell = 7$, orange for $\ell = 8$, and red for $\ell > 8$.

The observed excess of the number of IRs in most of the complete genomes of eubacteria cannot be due to a statistical fluctuation. Hence, it is important to relate this statistical observation to known biological functions. One explanation of the abundance of such inverted repeats in eubacteria is that they are used to code rho-independent hairpin in RNA during protein transcription [15,21,23,24]. Motivated by this fact, we investigate the location of each inverted repeats we find with respect to the biological information present in the annotation of each genome. The first investigation concerns the percentage of inverted repeats located in the non-coding DNA regions for each genome and for different values of the stem length $\ell \geq 6$. The results are summarized in Figure 2 where we show for each genome the ratio μ between the percentage of IRs found in non-coding regions and the percentage of non-coding regions present in the entire genome. Each vertical line refers to a genome. The grouping of genomes and their sequence is the same as the one given in Table I. Different colors refer to different values of ℓ . Specifically, we use green squares for $\ell = 6$, blue squares for $\ell = 7$, orange squares for $\ell = 8$, and red squares for $\ell > 8$. A null random hypothesis would suggest that $\mu \approx 1$ for all values of ℓ . Several genomes of groups II, III, IV and V show values of μ which are much larger than one. The value of μ always increases when ℓ increases assuming largest values for large values of ℓ . For most genomes, this implies that a large number of inverted repeats are almost exclusively located in the non-coding regions when the stem length is longer than 8. However, this behavior is not so pronounced in all investigated genomes. It is worth noting that the in-

verted repeats of most archaeobacteria are characterized by moderately large values of μ (see group I in Figure 2). Moreover, this different behavior is also observed for some eubacteria such as, for example, *Mycobacterium tuberculosis*, and *Treponema pallidum*.

A more quantitative test is obtained by performing a χ^2 test of the null hypothesis that the number of IRs found in non-coding regions is proportional to the percentage of non-coding regions present in the entire genome. The p -values associated to the above χ^2 test for $\ell = 6$ are below 1% confidence level in all but three genomes, specifically *Aeropyrum pernix*, *Pseudomonas aeruginosa* and *Treponema pallidum*. For IRs with stem length $\ell > 8$ only *Halobacterium* sp. and *Treponema pallidum* have a p -value larger than 1%. This test shows that for all the value of ℓ considered the IRs are preferentially located in non-coding DNA.

Non-coding regions of complete genomes can be classified with respect to the orientation of the bounding coding regions. Coding regions can be “divergent” (two 5’ ends bounding the non-coding region), “unidirectional” (examples are a spacer between two genes in one operon or a spacer between two consecutive unidirectional operons) or “convergent” (two 3’ ends bounding the non-coding region). The analysis of the statistical location of IRs in these biologically different non-coding regions provides relevant information about the potential biological role of some of the detected IRs. To perform a statistical analysis of the location of IRs in these three types of spacer we split the set of the non-coding regions in three subsets: (i) non-coding regions between two 5’ ends of two “divergent” genes (we address these non-coding regions as type A regions); (ii) non-coding regions between a 3’ end and a 5’ end of two different genes (type B regions) and (iii) non-coding regions between two 3’ ends of two “convergent” genes (type C regions). The genes bounding non-coding regions of type A and C certainly belong to two different operons, whereas the genes bounding non-coding regions of type B may or may not belong to the same operon. The statistical properties of the length of the non-coding regions are different for the three groups. The non-coding regions belonging to type A are in average longer than the non-coding regions belonging to the other two groups. A statistical characterization of all genomes shows that in (almost) all the considered genomes the probability density function of the length of non-coding regions of type A shows a broad maximum at a length of 150-200 nucleotides and decays to zero for small and large values of non-coding region length. The probability density function of length of non-coding regions belonging to type B is an exponentially decaying function approximately. The non-coding regions belonging to type C behave differently in genomes of different organisms. In many purple bacteria the probability density function of length of non-coding regions has a sharp peak located

at a length of 40-60 nucleotides approximately, whereas in other genomes an approximately monotonic decaying behavior is observed.

We investigate the distribution of IRs in non-coding regions belonging to different groups A, B and C. We make the null hypothesis that the probability of having an IR in any non-coding part of the genome is just proportional to the length of that non-coding region. For example, the probability of finding an IR in a non-coding region belonging to type A is given by the total length of non-coding regions of this type divided by the total length of the non-coding regions of the genome. For each genome and for each value of ℓ ($\ell = 6, \ell = 7, \ell = 8$ and $\ell > 8$) we compute the p -value associated to the χ^2 test of the above null hypothesis. Table II shows these p -values for the considered genomes. We note that in archaeobacteria the IRs are distributed in the three groups of non-coding regions in good agreement with the null hypothesis. The only exception is the *Halobacterium* genome for $\ell = 6$ and $\ell > 8$. On the other hand, for many eubacteria the p -values are very small especially for longer IRs. In these genomes, a direct inspection of the number of inverted repeats located in each group of non-coding regions shows that the IRs tend to be preferentially located in non-coding regions of type C when $\ell > 8$ for the genomes disproving the null hypothesis. Low p -values are also observed for low values of ℓ (we compute p -values also for $\ell = 4$ and 5. They are not shown in Table II for lack of space but available on-line). The reason of these low p -values for low values of ℓ is different from the one for the large values of ℓ for most genomes. For example, most of the genomes (31 over 37) show that the number of IRs located in the type A non-coding regions is exceeding the number expected under the null hypothesis by a six percent in average for $\ell = 4$. This result suggests a potential biological role of short IRs located in type A non-coding regions which is different from the biological role of long IRs located in type C non-coding regions.

Next we investigate the statistical properties of the distance of the IRs located in non-coding regions from the nearest coding region. This investigation is performed by dividing IRs in 4 groups. The first two groups contain IRs located in type A and type C non-coding regions previously defined. IRs located in type A non-coding regions are denoted as A5’ whereas IRs located in type C non-coding regions are denoted C3’. IRs found in type B regions are divided in two subgroups depending on the condition that the considered IRs is closer to a 5’ end (we address this subset as B5’) or to a 3’ end (we address this subset as B3’).

For each group and for each value of stem length ℓ , we estimate the mean distance of IR from the closest coding regions. This is done by analysing the four groups of IRs separately. To obtain mean values which are statistically reliable for IRs characterized by both small and large values of ℓ , we perform our analysis on the six genomes

having the largest number of inverted repeats. These genomes are *Bacillus halodurans*, *Bacillus subtilis*, *Neisseria meningitidis* serogroup B, *Escherichia coli*, *Pseudomonas aeruginosa* and *Vibrio cholerae* Chr I. In Table III we summarize the average distance of the IRs from the closest gene boundary for the four groups described above for $\ell = 6$ and $\ell > 8$. We select these values of ℓ to limit the size of the Table and because they are representative of the behavior observed for small and large values of ℓ . From the Table we note that the average distance of the IRs from the nearest coding region decreases when two conditions are simultaneously fulfilled. The first is that the considered IR has a stem length longer than 8 nucleotides ($\ell > 8$) and the second is that the IR is nearby the 3' end of a coding regions. In fact, for the B3' subset we observe that the mean distance from the 3' end of the coding region decreases when ℓ increases from 6 to a value larger than 8 for all the considered genomes. The same behavior is observed in the C3' subset. Indeed in this last case the decrease of the mean distance is even more pronounced than in the previous one. On the contrary, when the IR is closer to a 5' end of the nearest coding region the mean distance remains approximately the same when ℓ increases from 6 to values larger than 8 both for the case A5' and for the case B5'. Only one exception to this general trend is detected. It is the case of IRs of *V. cholerae* Chr I in the B5' subset.

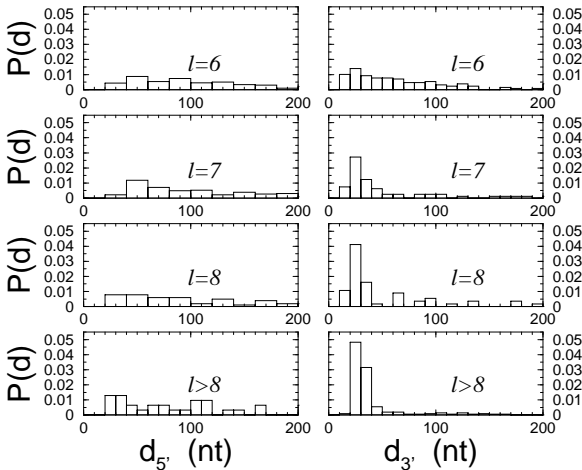


FIG. 3. Probability density functions $P(d)$ to find an IR nearby the 5' end of a coding region in a type A non-coding region (left panels) or an IR nearby the 3' end of a coding region in a type C non-coding region (right panels) when $\ell = 6$, $\ell = 7$, $\ell = 8$, and $\ell > 8$. Data refers to the complete genome of *E. coli*.

In Figure 3 we illustrate the decrease of the mean distance occurring for most eubacterial genomes rich of long inverted repeats by considering the case of *E. coli*. In the figure we show the empirical probability density functions $P(d)$ of (i) the distance d_5' , from a 5' end of an IR located

in a type A non-coding region (left panels) and (ii) the distance d_3' , from a 3' end of an IR located in a type C non-coding region (right panels) for $\ell = 6$, $\ell = 7$, $\ell = 8$, and $\ell > 8$. The left panels are always broad probability density functions not characterized by a sharp distance. In the right panels, the probability density function is also rather broad for $\ell = 6$. However, when ℓ increases above six $P(d_3')$ progressively displays a clear peak localized around $d_3' \approx 20$ nt. The preferential localization of the IRs characterized by a long stem nearby the 3' end of a coding regions supports the biologically motivated hypothesis that these structure may play the role of intrinsic terminators of the transcription process. However, the parallel analysis of 37 complete genomes summarized in Tables I and II shows that this is not a general feature of all bacteria but rather depends on the specific species

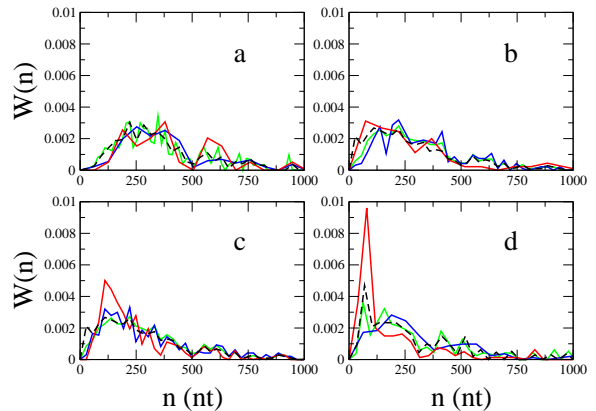


FIG. 4. Probability density function $W(n)$ of the length of the non-coding regions n in which an inverted repeat of stem length $\ell = 4$ (green line), $\ell = 6$ (blue line) and $\ell > 8$ (red line) is found. Data refers to the genome of *E. coli*. The black dashed line is obtained from the null random hypothesis discussed in the text. The four panels show the data for the four subsets of IRs defined in the text. Specifically, A5' IRs are in (a), B5' in (b), B3' in (c) and C3' in (d).

We have shown that for several eubacteria the average distance from the nearest coding region of IRs characterized by a large value of the stem length (usually $\ell > 8$) decreases when the IR is located nearby a 3' end of a coding regions. This behavior may be due to two different hypothesis. First, the longest IRs locate preferentially in short non-coding regions. Second, for each non-coding region of a given length the longest IRs belonging to subsets B3' and C3' tend to be located closer to the 3' end of the bounding gene than expected under a random assumption. The test of the second hypothesis is statistically difficult because the number of IRs is not sufficient to give a robust estimation of the mean distance of the IRs from the 3' end of the bounding gene conditioned to the length of the non-coding region in which the IR is found. For this reason, we test only the first hypothesis

in the present study. In order to test the first hypothesis we investigate the probability $W(n)$ that an IR, belonging to one of the four groups previously defined, is found in a non-coding region of length n . Specifically, for each IR found in non-coding DNA we associate the length of the non-coding region in which the IR is located. We determine the histogram of the length of the non-coding regions corresponding to each IR for the stem length $\ell = 4$, $\ell = 6$ and $\ell > 8$ for the four subsets A5', B5', B3' and C3'. This is shown in Figure 4 for the genome of *E. coli*. The used values of ℓ have been selected because they are representative of the behavior observed for small, medium and large values of the stem length. As a null hypothesis we assume that the probability that an IR, which is belonging to one of the four subsets, is found in a non-coding region of a length n is equal to the length of the non-coding region divided by the total length n_{tot} of the non-coding regions of the same type (A, B or C). The Figure 4 shows the probability density function expected according to this null hypothesis as a black dashed line. This reference probability density function

$$W(n) = A \frac{n}{n_{tot}} P(n) \quad (2)$$

is obtained by multiplying the empirical probability density function $P(n)$ of the length of non-coding regions measured in the corresponding group of regions times n/n_{tot} , i.e. the length of the non-coding region divided by the total length of non-coding regions belonging to the considered group. The parameter A is a normalizing constant. Panels (a) and (b) show that the probability density function $W(n)$ of IRs of subsets A5' and B5' is described quite well by the null hypothesis for all values of ℓ . Panel (c) shows that the probability density function $W(n)$ of IRs of subset B3' is in good agreement with the null hypothesis for $\ell = 4$ and $\ell = 6$ whereas a small discrepancy is observed for $\ell > 8$. This discrepancy becomes extremely evident in panel (d) which is showing $W(n)$ for IRs belonging to subset C3'. From the analysis of Figure 3 we conclude that long IRs located in a type C non-coding region are found in short non-coding regions with a much higher probability than expected from a null random hypothesis.

The final investigation concerns a comparison between the IRs found by us in the non-coding regions of several eubacteria and the intrinsic terminators predicted with bioinformatics methods in Ref. [24]. In this study the biological information summarized in the review paper of Ref. [15] are used to train a computer program able to detect potential rho-independent intrinsic terminators in DNA sequences. The optimization of the parameters of the program was performed to ensure that 89% of the rho-independent intrinsic terminators known from biological studies are identified by using the 98% confidence threshold. We have used the computer program TransTerm of Ref. [24] to detect how many of the IRs

with $\ell > 8$ we find in the non-coding regions of several eubacterial genomes are predicted as rho-independent terminators by TransTerm.

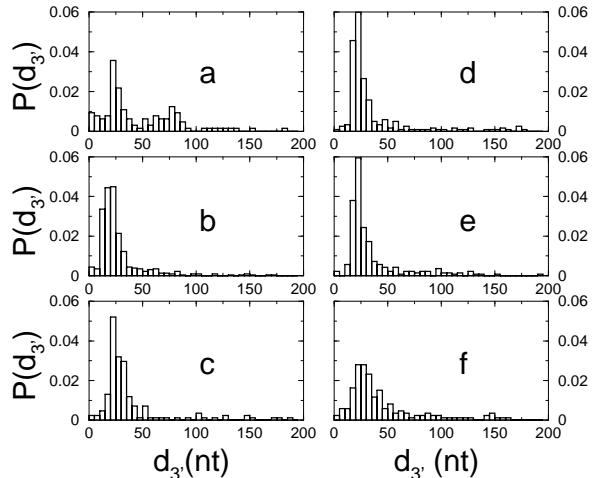


FIG. 5. Probability density function $P(d_{3'})$ of a subset of IRs with stem length $\ell > 8$ located in type B and C non coding regions. The subset is defined by considering the IRs which are nearby the 3' end of a coding region and which are not predicted as rho-independent intrinsic terminators by the TransTerm program at a 98% confidence threshold in the six genomes of (a) *Bacillus halodurans* (129 IRs), (b) *Bacillus subtilis* (459 IRs), (c) *Neisseria meningitidis* serogroup B (169 IRs), (d) *Escherichia coli* (241 IRs), (e) *Pseudomonas aeruginosa* (279 IRs) and (f) *Vibrio cholerae* (172 IRs).

By selecting the confidence level of 98% recommended by the authors, we note that only a part of the IRs localized nearby the end of the nearest coding regions are predicted as rho-independent terminators by TransTerm. Hundreds of IRs remain not predicted as potential rho-independent terminators by TransTerm. We verify that these IRs maintain the characteristic of being localized at a typical distance from the end of the nearest coding regions in several genomes very rich in IRs. Figure 5 shows the inverted repeats with $\ell > 8$ which are not predicted as rho-independent intrinsic terminators by TransTerm in the six genomes of *Bacillus halodurans*, *Bacillus subtilis*, *Neisseria meningitidis* serogroup B, *Escherichia coli*, *Pseudomonas aeruginosa* and *Vibrio cholerae*. In all these cases the IRs are still localized near the end of the nearest coding regions.

Conclusion

In summary, a comparative statistical investigation of the number and location of IRs in several different complete genomes shows that a large number of them may play a role in several eubacteria as intrinsic terminators of the transcription process. For almost all the bacteria

investigated, we quantitatively show that the IRs locates preferentially in non-coding regions. Moreover, in several eubacteria, IRs characterized by large values of the stem length ℓ locate preferentially in the non-coding regions bounded by two 3' ends of convergent genes. We also show statistical evidence that long IRs are found in short non-coding region more frequently than expected under a null random hypothesis. A large number of the IRs detected with our statistical methodology near the 3' end of a coding region are different from the rho-independent transcription terminators detected with a specialized computer program trained by using molecular biological information exclusively determined by investigating transcription process in *Escherichia coli*. Our findings based on the comparative analysis of non-coding regions of complete genomes suggest that other forms of intrinsic termination may be active in several eubacteria.

Inverted repeats are not only involved in transcription termination in bacteria. Indeed, by performing our comparative genomic study we are able to show that short IRs are slightly more abundant than expected under a null hypothesis in type A non-coding regions of several genomes. This may be due to nucleotide concentration fluctuation correlated to the type of non-coding region considered or may indicate a potential biological role of some of these short IRs consistent with known results of the literature [2–6]. The role of IRs with short values of ℓ located in type A non-coding regions will be considered in a future study.

ACKNOWLEDGMENTS

We thank INFM and MURST for financial support. We also wish to thank referees for useful remarks and interesting suggestions. This work is part of the INFM-PAIS project “Statistical modeling of non-coding DNA”.

-
- [1] Sinden,R.R. (1994) *DNA Structure and Function*. Academic Press, San Diego.
 - [2] Post,L.E., Reusser,F. and Nomura,M. (1978) DNA sequences of promoter regions for the *str* and *spc* ribosomal protein operons in *E. coli*. *Cell* **15**, 215–229.
 - [3] Shen,P., Zengel,J.M., and Lindahl,L. (1988) Secondary structure of the leader transcript from the *Escherichiacoli* S10 ribosomal protein operon. *Nucleic Acids Res.* **16**, 8905–8924.
 - [4] Li,X., Lindahl,L., Sha,Y. and Zengel,J.M. (1997) Analysis of the *Bacillussubtilis* S10 ribosomal protein gene cluster identifies two promoters that may be responsible for transcription of the entire 15-kilobase S10-*spc* - α cluster. *J. Bacteriol.* **179**, 7046-7054.
 - [5] Sadler,J.R., Sasmor,H. and Betz,J.L. (1983) A perfectly symmetric *lac* operator binds the *lac* repressor very tightly. *Proc. Natl. Acad. Sci. USA* **80**, 6785–6789.
 - [6] Simons,A., Tils,D., von Wilcken-Bergmann,B. and Müller-Hill,B. (1984) Possible ideal *lac* operator: *Escherichiacolilac* operator-like sequences from eukaryotic genomes lack the central *G·C* pair. *Proc. Natl. Acad. Sci. USA* **81**, 1624–1628.
 - [7] Raghunathan, G., Jernigan, R.L., Miles, H.T. and Sasisekharan, V. (1991) Conformational feasibility of a hairpin with two purines in the loop. *Biochemistry* **30**, 782–788.
 - [8] Blatt,N.B., Osborne,S.E., Cain,R.J. and Glick,G.D. (1993) Conformational studies of hairpin sequences from the ColE1 cruciform. *Biochimie* **75**, 433–441.
 - [9] Wadkins,R.M. (2000) Targeting DNA secondary structures. *Current Medicinal Chemistry* **7**, 1–15.
 - [10] Farnham,P.J. and Platt,T. (1981) Rho-independent termination: dyad symmetry in DNA causes RNA polymerase to pause during transcription in vitro. *Nucl. Acids Res.* **9**, 563–577.
 - [11] Platt, T. (1986) Transcription termination and the regulation of gene expression. *Ann. Rev. Biochem.* **55**, 339–372.
 - [12] Yager,T.D. and von Hippel,P.H. (1991) A thermodynamic analysis of RNA transcript elongation and termination in *Escherichia coli*. *Biochemistry* **30**, 1097–1118.
 - [13] Kroll,J.S., Loynds,B.M. and Langford,P.R. (1992) Palindromic haemophilus DNA uptake sequences in presumed transcriptional terminators from *H. influenzae* and *H. parainfluenzae*. *Gene* **114**, 151–152.
 - [14] Wilson,K.S. and von Hippel,P.H. (1995) Transcription termination at intrinsic terminators: the role of the RNA hairpin. *Proc. Natl. Acad. Sci. USA* **92**, 8793–8797.
 - [15] Carafa,Y.D., Brody,E. and Thermes,C. (1990) Prediction of Rho-independent *Escherichia coli* transcription terminators. *J. Mol. Biol.* **216**, 835–858.
 - [16] Diaz,E. and Garcia,J.L. (1990) Characterization of the transcription unit encoding the major pneumococcal autolysin. *Gene* **90**, 157–162.
 - [17] Gamper,M., Ganter,B., Polito,M.R. and Haas,D. (1992) RNA processing modulates the expression of the *arc*dabc operon in *Pseudomonas aeruginosa*. *J. Mol. Biol.* **226**, 943–957.
 - [18] Kimsey,H.H. and Kaiser,D. (1992) The orotidine-5'-monophosphate decarboxylase gene of *Myxococcus xanthus* - comparison to the *omp* decarboxylase gene family. *J. Biol. Chem.* **267**, 819–824.
 - [19] Steiner,K. and Malke,H. (1997) Primary structure requirements for in vivo activity and bidirectional function of the transcription terminator shared by the oppositely oriented *skc*/*rel-orf1* genes of *Streptococcus equisimilis* H46A. *Mol. Gen. Genet.* **255**, 611–618.
 - [20] Pattaragulwanit, K., Brune, D.C., Truper, H.G. and Dahl, C. (1998) Molecular genetic evidence for extracytoplasmic localization of sulfur globules in *Chromatium vinosum*. *Arch. Microbiol.* **169**, 434–444.
 - [21] Schroth,G.P., and Shing Ho,P. (1995) Occurrence of potential cruciform and H-DNA forming sequences in genomic DNA. *Nucleic Acids Res.* **23**, 1977–1983.
 - [22] Smith, H.O., Tomb, J.-F., Dougherty, B.A., Fleis-

- chmann, R.D. and Venter, J.C. (1995) Frequency e distribution of DNA uptake signal sequences in the *Haemophilus influenzae* Rd genome. *Science* **269**, 538–540.
- [23] Cox,R. and Mirkin,S.M. (1997) Characteristic enrichment of DNA repeats in different genomes. *Proc. Natl. Acad. USA* **94**, 5237–5242.
- [24] Ermolaeva,M.D., Khalak,H.G., White,O., Smith,H.O. and Salzberg,S.L. (2000) Prediction of transcription terminators in bacterial genomes. *J. Mol. Biol.* **301**, 27–33 (2000).

TABLE I. Inverted repeats per million base pair of stem length ℓ and loop length within the interval $3 \leq m \leq 10$ detected in 37 complete genomes.

Genome	$\ell = 6$	$\ell = 7$	$\ell = 8$	$\ell > 8$
<i>A. pernix</i>	1519.44 (1388.88)	444.39 (344.97)	116.19 (110.20)	45.52 (26.95)
<i>A. fulgidus</i>	1387.72 (1325.74)	302.52 (331.89)	94.11 (81.71)	25.71 (34.89)
<i>Halobacterium</i> sp.	2893.40 (2450.06)	938.32 (728.31)	328.66 (215.96)	171.78 (86.88)
<i>M. jannaschii</i>	2258.90 (2378.42)	706.32 (689.50)	219.82 (211.42)	137.54 (81.08)
<i>M. thermoautotrophicum</i>	1573.62 (1272.71)	435.66 (341.45)	108.49 (80.51)	34.83 (23.98)
<i>P. abyssi</i>	1291.13 (1328.52)	339.35 (328.59)	92.91 (83.28)	39.66 (31.16)
<i>P. horikoshii</i>	1396.03 (1414.43)	371.58 (389.99)	101.81 (104.69)	48.32 (40.84)
<i>T. acidophilum</i>	1455.68 (1229.47)	398.11 (318.87)	114.38 (78.60)	46.65 (34.51)
<i>C. pneumoniae</i> AR39	1916.49 (1428.63)	541.53 (366.71)	187.83 (94.32)	135.79 (31.71)
<i>C. pneumoniae</i> CWL029	1915.90 (1402.99)	541.36 (403.99)	188.58 (101.61)	132.50 (24.39)
<i>C. pneumoniae</i> J138	1921.41 (1465.48)	538.16 (381.84)	188.88 (86.30)	135.15 (33.38)
<i>C. trachomatis</i>	1997.36 (1439.11)	575.08 (401.16)	205.72 (98.18)	165.51 (29.92)
<i>C. trachomatis</i> ser D	1956.80 (1391.82)	638.84 (335.73)	195.68 (95.92)	175.54 (34.53)
<i>B. halodurans</i>	1415.16 (1289.04)	376.69 (340.29)	103.04 (90.90)	143.02 (32.36)
<i>B. subtilis</i>	1492.83 (1408.13)	404.76 (355.41)	121.95 (101.07)	216.14 (28.47)
<i>M. genitalium</i>	3192.70 (2628.98)	1030.90 (656.81)	330.99 (237.90)	160.32 (89.64)
<i>M. pneumoniae</i>	2163.17 (1618.09)	608.77 (436.06)	224.16 (104.12)	107.79 (53.90)
<i>U. urealyticum</i>	4244.94 (3824.57)	1416.75 (1219.87)	525.46 (401.75)	323.26 (183.58)
<i>M. tuberculosis</i>	2179.97 (1947.85)	638.55 (560.80)	202.20 (158.45)	100.87 (56.67)
<i>R. prowazekii</i>	3131.74 (2724.19)	957.25 (853.78)	287.89 (229.41)	166.44 (103.46)
<i>N. meningitidis</i> ser A	1649.88 (1463.56)	432.61 (397.36)	417.96 (96.14)	231.64 (39.37)
<i>N. meningitidis</i> ser B	1648.07 (1419.68)	462.52 (375.38)	415.43 (94.62)	239.40 (34.77)
<i>C. jejuni</i>	3334.18 (2939.42)	1019.81 (883.35)	339.33 (252.82)	226.62 (122.45)
<i>H. pylori</i> 26695	2159.04 (1960.59)	585.78 (549.80)	204.45 (175.07)	90.53 (65.35)
<i>H. pylori</i> J99	2101.19 (1885.84)	605.29 (537.16)	184.33 (147.22)	83.34 (55.97)
<i>Buchnera</i> sp.	4807.38 (3469.75)	1793.40 (1052.01)	616.53 (334.02)	358.99 (163.89)
<i>E. coli</i>	1441.62 (1216.58)	419.90 (322.04)	147.22 (76.52)	154.98 (27.16)
<i>H. influenzae</i>	2015.69 (1748.50)	596.13 (469.36)	181.95 (139.88)	204.36 (62.84)
<i>P. aeruginosa</i>	2422.58 (2072.34)	740.37 (563.02)	251.74 (167.29)	182.30 (58.90)
<i>V. cholerae</i> Chr I	1508.87 (1266.40)	414.37 (323.19)	136.77 (85.10)	215.79 (29.04)
<i>X. fastidiosa</i>	1391.03 (1155.52)	397.12 (301.20)	103.01 (74.65)	76.51 (27.99)
<i>A. aeolicus</i>	1489.68 (1518.69)	415.77 (384.83)	107.00 (109.58)	35.45 (35.45)
<i>B. burgdorferi</i>	3235.89 (2847.19)	1068.38 (908.07)	332.70 (311.84)	262.43 (124.08)
<i>T. pallidum</i>	1539.53 (1213.52)	424.42 (304.04)	100.17 (76.45)	69.42 (21.09)
<i>D. radiodurans</i>	1545.32 (2050.11)	345.46 (584.83)	81.93 (161.59)	62.30 (65.32)
<i>Synechocystis</i> sp.	1096.13 (1379.61)	223.59 (378.34)	47.01 (94.59)	12.03 (36.94)
<i>T. maritima</i>	1609.05 (1399.99)	447.14 (382.65)	140.81 (107.48)	116.62 (25.26)

The number in parenthesis is the theoretical prediction obtained from computer data generated by using a local first-order Markov process. We use the color code described in the text to quantify the discrepancy between the empirical results and the predictions of the Markov model.

TABLE II. p -values associated with the χ^2 test of the null hypothesis discussed in the text on the distribution of inverted repeats in the different types of non-coding regions for 37 bacterial genomes.

<i>Genome</i>	$l = 6$	$l = 7$	$l = 8$	$l > 8$
<i>A. pernix</i>	69.68	49.54	78.37	82.65
<i>A. fulgidus</i>	25.53	44.92	6.75	75.39
<i>Halobacterium</i>	0.47	19.94	61.33	0.33
<i>M. jannaschii</i>	42.14	2.33	3.09	90.29
<i>M. thermoautotrophicum</i>	2.16	28.95	2.66	88.31
<i>P. abyssi</i>	54.75	7.50	3.23	41.93
<i>P. horikoshii</i>	6.59	23.62	70.80	39.27
<i>T. acidophilum</i>	5.80	2.50	27.14	69.38
<i>C. pneumoniae</i> AR39	10.70	37.87	6.16	8.28
<i>C. pneumoniae</i> CWL029	1.38	12.45	11.98	4.35
<i>C. pneumoniae</i> J138	7.01	29.77	42.17	0.00
<i>C. trachomatis</i>	70.56	79.23	89.88	0.00
<i>C. trachomatis</i> ser D	0.85	48.25	95.20	0.00
<i>B. halodurans</i>	10.10	50.04	88.75	0.00
<i>B. subtilis</i>	8.03	49.84	1.72	0.00
<i>M. genitalium</i>	97.27	23.22	22.19	24.69
<i>M. pneumoniae</i>	11.97	60.14	38.18	28.93
<i>U. urealyticum</i>	0.18	21.55	9.51	0.48
<i>M. tuberculosis</i>	86.16	23.36	70.71	3.73
<i>R. prowazekii</i>	2.19	58.18	88.54	87.07
<i>N. meningitidis</i> ser A	13.71	21.99	0.00	0.00
<i>N. meningitidis</i> ser B	0.33	0.08	0.00	0.00
<i>C. jejuni</i>	0.02	49.08	93.59	0.00
<i>H. pylori</i> 26695	17.32	0.04	97.81	11.29
<i>H. pylori</i> J99	28.40	87.26	73.48	0.01
<i>Buchnera</i> sp.	0.03	4.37	42.02	11.16
<i>E. coli</i>	3.06	0.16	0.00	0.00
<i>H. influenzae</i>	0.86	38.33	0.20	0.00
<i>P. aeruginosa</i>	1.54	0.00	0.00	0.00
<i>V. cholerae</i> Chr I	0.64	19.41	0.00	0.00
<i>X. fastidiosa</i>	78.58	35.77	17.10	2.02
<i>A. aeolicus</i>	69.94	32.28	24.83	66.97
<i>B. burgdorferi</i>	0.01	14.34	25.77	0.00
<i>T. pallidum</i>	21.35	91.15	0.99	6.45
<i>D. radiodurans</i>	0.03	0.00	0.03	0.00
<i>Synechocystis</i> sp.	1.46	40.93	1.59	33.15
<i>T. maritima</i>	20.98	27.83	2.59	0.00

TABLE III. Mean distance of the inverted repeats from the closest gene boundary for the four groups of inverted repeats defined in the text for six bacterial genomes.

<i>Genome</i>	A5'		B5'		B3'		C3'	
	$l = 6$	$l > 8$	$l = 6$	$l > 8$	$l = 6$	$l > 8$	$l = 6$	$l > 8$
<i>B. halodurans</i>	97.41	111.2	106.3	106.1	84.49	56.28	67.34	30.59
<i>B. subtilis</i>	86.84	81.90	78.82	83.79	61.96	30.12	79.75	25.86
<i>E. coli</i>	99.71	89.64	85.96	80.00	74.41	39.31	80.85	32.19
<i>N. meningitidis</i> ser B	100.9	83.19	123.5	100.7	97.46	41.47	154.0	48.92
<i>P. aeruginosa</i>	91.26	117.0	76.01	77.64	66.04	38.87	80.46	35.95
<i>V. cholerae</i> Chr I	93.39	110.7	95.52	40.96	62.61	38.90	84.62	41.86